

# High-Impedance Fault Identification Using Cyclostationary Characteristic Analysis

F. P. Souza, L. F. Q. Silveira, F. B. Costa, M. M. Leal

**Abstract**—Conventional overcurrent-based protection systems are generally not sensitive to high impedance faults (HIFs) since they have a low overcurrent amplitude. This type of fault causes damages to dealers and can provoke the deaths of people and animals. Therefore, different methods for identifying HIFs in electric power distribution systems have been proposed. However, besides the low fault overcurrent level be still a problem, the noise interference on signals is also a difficulty for non-conventional methods. Therefore, this work proposes a reliable method based on statistical characteristics for identifying HIFs regardless of the noise interference and the overcurrent level. Specifically, the method uses cyclostationary characteristic analysis to extract cyclic autocorrelation information from the signals of interest by calculating the cyclic spectral density function. From this information, HIFs can be properly identified among other power system disturbances. The performance of the method was assessed with actual HIF data and with realistic HIF simulations, presenting promising results.

**Index Terms**—High impedance fault, cyclostationary analysis, alpha profile, distribution systems.

## I. INTRODUCTION

**T**HE contact between a downed energized overhead conductor and a high impedance surface causes HIFs in electrical power distribution systems. The contact of an energized overhead conductor with trees also produces HIFs [1]. Power utilities need reliable methods to detect and identify HIFs to protect the distribution systems and their equipment and maintain the continuity of the power supply. Notwithstanding, power utilities have to prevent a possibly fatal accident to people and animals due to the contact with downed-energized conductors. For instance, the number of reported accidents in Brazilian distribution systems was 891 in 2018, according to the Brazilian Association for the Distribution of Electric Energy (ABRADEE). The number of deaths was 271. The second-largest cause of fatalities was an accident involving ruptures of energized conductors to the ground or contact with a tree, resulting in HIFs, totaling 31 deaths (11% of total the total deaths) [2]. Therefore, the development of HIF detection and identification methods is primordial to the distribution system.

Signal processing techniques and artificial intelligence have been employed to detect/identify HIFs, such as the discrete

wavelet transform [3], [4], boundary wavelet transform [1], Fourier-based transforms [5], mathematical morphology [6], [7], Kalman extended filters [8] as well as artificial intelligence and fuzzy logic [9]–[11]. The main problems faced by these methods are: 1) the low current magnitude of HIFs; 2) the noise; 3) inner HIF features such as intermittence, build-up, shoulder, non-linearity, and harmonic distortions, which are also present in other events such as transformer energization, capacitor bank switching, and non-linear loads; 4) actual data with HIFs are difficult to be obtained since actual devices are not sensitive to most HIFs, which difficult the development of HIF detection and identification methods; 5) and challenging to identify an accurate HIF model for simulation. Since the development of an accurate HIF detection and identification method is still a critical point today, the need to testify new techniques that were never used for this purpose is evident.

Cyclostationary analysis has been successfully used in different areas, such as telecommunications, hydrology, meteorology, biology, aeronautics, medicine, among others [12]–[14]. Its principal property is its immunity to high noise levels, which would help the power system disturbance diagnosis. However, for the best of the author's acknowledgment, there is no application of it in the power system disturbance detection reported in the literature.

This work proposes an efficient and reliable method based on the cyclostationary technique to identify HIFs regardless of the noise interference and the overcurrent level, overcoming significant limitations of most existing methods. Firstly, the proposed method uses an existing method to detect a transient disturbance as a previous step [1]. Therefore, HIFs, faults, and other transient disturbances are adequately detected. After the detection, a spectral cyclic density function (SCD) generates an alpha profile from the analyzed signal. After that, a HIF is identified with the comparison of the alpha profile with some templates, which were obtained from actual HIFs. If the HIF is not recognized, then the method generates an alert flag informing the presence of other disturbances. The proposed method was evaluated with simulated HIFs from accurate models, achieving outstanding results. Besides, actual HIFs validated the effectiveness of the proposed method.

## II. CYCLOSTATIONARY CHARACTERISTICS ANALYSIS

Classical statistical methods treat random signals as stationary, whether its statistical parameters do not vary with time. However, many human-made signals found in electrical and electronic systems and natural origins signals have second-order statistics that vary periodically in time ( $t$ ) due to the intrinsic variation of fundamental physical mechanisms that

This study was financed in part by the Coordenação de Aperfeiçoamento de Pessoal de Nível Superior - Brasil (CAPES) - Finance Code 001 and in part by the Conselho Nacional de Desenvolvimento Científico e Tecnológico - Brasil (CNPq).

F. P. Souza, L. F. Q. Silveira, F. B. Costa, M. M. Leal are with Federal University of Rio Grande do Norte (UFRN), Campus Universitário Lagoa Nova, Natal - RN, 59.078-970, Brazil (e-mail:frankeleneps@gmail.com, lfe-lipe@dca.ufrn.br,flaviocosta@ect.ufrn.br,monicamleal@gmail.com).

Paper submitted to the International Conference on Power Systems Transients (IPST2021) in Belo Horizonte, Brazil June 6-10, 2021.

generate these signals. Therefore, the performance of signal processing techniques can be improved by recognizing and exploiting this latent periodicity, which can be achieved by modeling the signal as second-order cyclostationary, which means that its mean  $E\{x(t)\}$  and autocorrelation  $R_x(t, \tau) \triangleq E\{x(t+\tau)x^*(t)\}$  are periodic functions in  $t$  to every  $\tau$ , with period  $T$  [15].

#### A. Cyclic Autocorrelation Function - CAF

Since the autocorrelation function  $R_x(t, \tau)$  of a second-order cyclostationary signal is periodic in  $t$ , it can be expanded in Fourier series as follows [12]:

$$R_x(t, \tau) = \sum_{\alpha} R_x^{\alpha}(\tau) e^{j2\pi\alpha t}, \quad (1)$$

where  $\alpha = \{n/T\}_{n \in \mathbb{Z}}$  is called cyclic frequency, measured in Hz, which represents all multiples of the fundamental frequency. In this context, the Fourier series coefficients define the Cyclic Autocorrelation Function (CAF) as follows:

$$R_x^{\alpha}(\tau) \triangleq \lim_{T \rightarrow \infty} \frac{1}{T} \int_{-T/2}^{T/2} R_x(t, \tau) e^{-j2\pi\alpha t} dt. \quad (2)$$

The CAF can also be interpreted as an analytical function that verifies when the process  $x(t)$  is cyclostationary by evaluating whether  $R_x^{\alpha}(\tau)$  is non-null for any  $\alpha \neq 0$ .

#### B. Spectral Cyclic Density Function - SCD

The cyclic Wiener-Khinchin relation [16] can be used to define the Spectral Cyclic Density (SCD) function as the Fourier transform of the CAF, thus:

$$S_x^{\alpha}(f) \triangleq \int_{-\infty}^{\infty} R_x^{\alpha}(\tau) e^{-j2\pi f \tau} d\tau \quad (3)$$

$$= \lim_{W \rightarrow \infty} \lim_{Z \rightarrow \infty} \frac{1}{Z} \int_{-Z/2}^{Z/2} \frac{1}{W} E\{X_W(t, f) \times X_W^*(t, f - \alpha)\} dt, \quad (4)$$

where

$$X_W(t, f) \triangleq \int_{t-W/2}^{t+W/2} x(u) e^{-j2\pi f u} du \quad (5)$$

is the Short-Time Fourier Transform (STFT) over the time interval  $[t-W/2; t+W/2]$ , where  $W$  is the STFT observation length, and  $Z$  is the total observation length [15].

Assuming ergodic signals, the time average can be used to estimate the SCD function, as follows [15]:

$$S_x^{\alpha}(f) = \left\langle X_W \left( t, f + \frac{\alpha}{2} \right) X_W^* \left( t, f - \frac{\alpha}{2} \right) \right\rangle_t, \quad (6)$$

where  $\langle \cdot \rangle_t$  is defined by:

$$\langle \cdot \rangle_t \triangleq \lim_{T \rightarrow \infty} \frac{1}{T} \int_{-T/2}^{T/2} (\cdot) dt. \quad (7)$$

The cyclostationary characteristics of a signal depend on the underlying stochastic process that originated the signal. Therefore, cyclostationary analysis functions, such as SCD, can be used to classify these processes.

#### C. Alpha profile

The SCD function is a surface defined on the bi-frequency plane  $(\alpha, f)$ , i.e., a three-dimensional representation. However, this surface can be reduced without losing relevant information to a two-dimensional representation, called  $\alpha$ -profile, which presents the maximum value set of the SCD function on a plane orthogonal to  $f$ , for each value of  $\alpha$  [17].

#### D. Cyclic Periodogram Detection Algorithm

The cyclic periodogram detection (CPD) algorithm [18] can be used to estimate the SCD based only on the sampled signal  $x[n]$ . The following steps describe this algorithm:

- The input signal is divided in  $L$  blocks of  $N$  samples each, denoted  $x_l[n]$ , where  $n = 0, 1, 2, \dots, N-1$  and  $l = 0, 1, 2, \dots, L-1$ .
- The discrete Fourier transform of each  $l$ -th block employs the radix-2 fast Fourier transform (FFT) algorithm:

$$X_l[k] = \sum_{n=0}^{N-1} x_l[n] e^{-j\frac{2\pi}{N}kn}, \quad k = 0, 1, \dots, N-1. \quad (8)$$

- The cyclostationary features are obtained from each block, according to the following expression:

$$T_l^{\alpha}[k] = \frac{1}{N} X_l \left[ k + \frac{\alpha}{2} \right] X_l^* \left[ k - \frac{\alpha}{2} \right]. \quad (9)$$

- The mean value of  $T_l^{\alpha}[k]$  is computed from the all  $L$  blocks:

$$T^{\alpha}[k] = \frac{1}{L} \sum_{l=0}^{L-1} T_l^{\alpha}[k], \quad k = 0, 1, 2, \dots, N-1. \quad (10)$$

- $T^{\alpha}[k]$  is then frequency-smoothed to give the cyclic periodogram:

$$S^{\alpha}[k] = \frac{1}{M} \sum_{m=0}^{M-1} T^{\alpha}[kM + m]. \quad (11)$$

#### E. Computational Burden of the CPD Algorithm

The number of floating-point operations (FLOPs) required by the proposed CPD algorithm is an important parameter to verify if the proposed method is feasible to be implemented in hardware for a real-time evaluation in a practical application. Table I summarizes the number of floating-point additions and multiplications necessary for calculating Eqs. (8)-(11). This analysis considers a signal  $x[n]$  formed by  $L$  blocks, each of them with  $N$  samples. The total computational burden of the proposed CPD algorithm is  $LN(4N + 3 \log_2 N) + N(N+1)$  FLOPs.

TABLE I  
CPD ALGORITHM: NUMBER OF FLOATING-POINT OPERATIONS.

	Additions	Multiplications
Eq. (8)	$2LN \log_2 N$	$LN \log_2 N$
Eq. (9)	—	$3LN^2$
Eq. (10)	$(L-1)N^2$	$N^2$
Eq. (11)	$\frac{N^2(M-1)}{M}$	$N(\frac{N}{M} + 1)$

### III. TRANSIENT DISTURBANCE DETECTION METHOD

The proposed method is triggered through a disturbance detection method based on the analysis of the first level wavelet coefficient energy of currents proposed by [1]. This method is not able to identify HIFs. However, it is sensible to transients induced by faults, HIFs, and switching operations. Therefore, this method triggers the proposed method when any transient disturbance is detected.

The disturbance detection method to trigger the proposed method is out of the scope of this paper, and any detector could be used. Therefore, details about the transient disturbance detection method can be found in [1], and just a brief review of it is presented in this section.

The first level boundary wavelet coefficients of the Daubechies mother wavelet with four coefficients (db(4)) associated in time to  $k/f_s$  are computed through inner products between the four coefficients of the wavelet filter ( $h = \{-0.1294, -0.2241, 0.8365, -0.4830\}$ ) and four samples of the time-domain current signal ( $i$ ) inside a circular sliding window with length  $\Delta k$  as follows [19]:

$$w_{db4}(l, k) = \frac{1}{\sqrt{2}} \sum_{n=0}^3 h(n) \hat{i}(k + n + l - 3), \quad (12)$$

where  $0 \leq l < L$ ;  $L \leq \Delta k$ ;  $k \geq \Delta k - 1$ ;  $\hat{i}(k + m) = i(k - \Delta k + m)$  for any integer  $m$  (periodized signal in  $\Delta k$  samples).

The one-cycle wavelet coefficient energy ( $\mathcal{E}^w$ ), at the first scale, is given by [20], [21]:

$$\mathcal{E}^w(k) = \sum_{l=1}^3 [w_{db4}(l, k)]^2 + \sum_{n=k-\Delta k+3}^k [w_{db4}(0, n)]^2, \quad (13)$$

where  $k \geq \Delta k - 1$  and  $\Delta k = f_s/f$  is the one-cycle window.

Based on [1], reference energy is defined as the average energy in one cycle during the steady-state period, which is adapted to the noise level of the currents. Therefore, a HIF or other transient disturbance is detected when the energy  $\mathcal{E}^w$  is higher than twice the reference energy for more than one-cycle duration.

### IV. THE PROPOSED HIF IDENTIFICATION METHOD

Fig. 1 depicts the flowchart of the proposed method. Firstly, it is necessary to present currents from the distribution power system to the proposed method. The currents might be measured in distribution lines or in distribution substations through current transformers. The proposed method can be used in an offline analysis just with oscillographic records, whereas in a real-time evaluation it is necessary a hardware implantation.

As aforementioned, the method presented in [1] detects the inception time of transient disturbances, such as faults, HIFs, inrush currents, and other events. Despite being unable to identify a HIF, the wavelet-based detection method is used to trigger the proposed method, which identifies a HIF through the analysis of cyclostationary characteristics, as shown in Fig. 1. The CPD algorithm is then executed, obtaining the  $\alpha$  profile of the analyzed currents. A classifier uses this  $\alpha$  profile to identify a HIF. The quality descriptors obtained through

CPD lead to a simple classification scheme to guarantee good success rates in identifying HIFs. The steps in this flow chart are described in the remainder of this section.

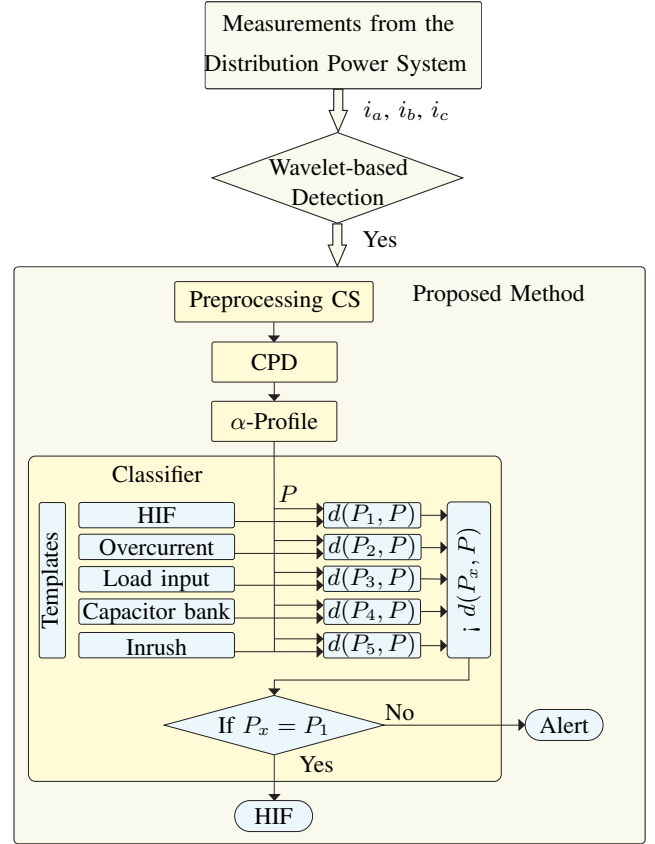


Fig. 1. The proposed HIF identification method.

#### A. Detection of onset of disturbance

The wavelet coefficient energy is used to detect the beginning of the transients. When a disturbance occurs, the energy rises even under high noise and low inception angle due to the boundary effect. Once the transient detection occurs by using [1], the HIF identification is analyzed using cyclostationary characteristics.

#### B. Pre-processing

The proposed method implementation requires a down-sampling of the original current signal. The signal sampling frequency influences the distribution of the cyclic frequencies. Tests were performed to verify which sampling frequency has the best result, and it was verified that when resampling the signal at 720 Hz, the cyclostationary characteristics in the  $\alpha$  profile became more discriminative. Therefore, the current of the analyzed signal is resampled at a frequency of 720 Hz, containing the fundamental component, the 3<sup>o</sup> and 5<sup>o</sup> harmonic components.

#### C. Alpha Profile

The  $\alpha$ -profiles from currents were generated to different disturbances presented in the distribution system. Specifically,

$\alpha$ -profiles were obtained to HIF, overcurrent faults, load input, capacitor bank switching, and transformer energization, corresponding to the inrush current. The  $\alpha$ -profiles were normalized by using the amplitude as reference. The  $\alpha$ -profiles present distinct features to each type of evaluated disturbance. Therefore, when a disturbance is detected in the system, the  $\alpha$ -profile of the current signal is estimated employing the CPD algorithm. The cyclic characteristics evidenced by the  $\alpha$ -profiles are used in the classification stage.

#### D. Classification

HIF identification is made through the analysis of the cyclostationary characteristic. The statistical characteristics from the distributed system current signals are extracted by using the SCD function. The generated descriptors are classified through their cyclostationary characteristics. Therefore, the proposed classifier is defined employing the smaller Euclidean distance between the  $\alpha$ -profile of the analyzed signal and the  $\alpha$ -profile references, which are defined as templates to each type of considered disturbance.

The Euclidean distance can be used as a measure of similarity between the analyzed signal  $\alpha$ -profile and the profile of each template, which represents a disturbance in the distribution system, given by [22]:

$$d(P(x), P) = \sqrt{\sum_{i=1}^n (P(x)_i - P_i)^2}, \quad (14)$$

where  $P$  represents the analyzed signal  $\alpha$  profile and  $P(x)$  denotes the  $x$ -th template, both with  $n$  samples.

The greater the similarity of the  $\alpha$  profiles is, the shorter the Euclidean distance is. Once the templates are defined, a comparison of the calculated distances is made. The template associated with the shortest distance indicates the type of disturbance the distribution system is perceived.

The decision block receives the value of the shortest Euclidean distance associated with a given  $\alpha$  profile ( $Px$ ). If  $Px$  is the template associated with HIF, the trip is sent to breaker informing the occurrence of a HIF in the distribution system. Otherwise, an alert is issued, which represents the presence of other disturbances in the system.

### V. PERFORMANCE EVALUATION

The performance of the proposed method was evaluated by using simulations from two different distribution test systems, using simulation data from a modeled IEEE 30-bus distribution system and using actual data from a Brazilian distribution system. The noise influence was carefully evaluated by the proposed method. Besides, the proposed method performance was compared to a traditional overcurrent protection.

#### A. Performance Assessment with Actual HIF Data

The proposed method performance was evaluated with 57 actual HIF currents which took place on different contact ground surfaces, such as sand, asphalt, gravel, and pavement in a distribution power system. The HIFs took place in both

wet and dry ground surfaces. Fig. 2 depicts some examples of actual HIF currents for different contact surfaces: sand, gravel, asphalt, and pavement in the left-hand side with their respective  $\alpha$  profiles in the right-hand side. The  $\alpha$  profiles were normalized with the highest cyclical frequency.

The HIF currents in Fig. 2 (left-hand side) present different shapes because HIFs present random phenomena, even considering the same ground surface. In addition, most HIFs do not present relevant overcurrent, which make HIFs difficult events to be detected. However, HIFs present invariant cyclostationary characteristics in the domain of cyclic frequency such as shown in the right-hand plots in Fig. 2. In addition, the cyclostationary characteristics are scarcely affected by the overcurrent and noise levels, overcoming the main limitations of HIF detection methods. Considering all the 57 actual HIFs, the related  $\alpha$  profile presented peaks in the expected cyclic frequencies. Therefore, the proposed method presented a 100% of success rate in the identification of actual HIFs.

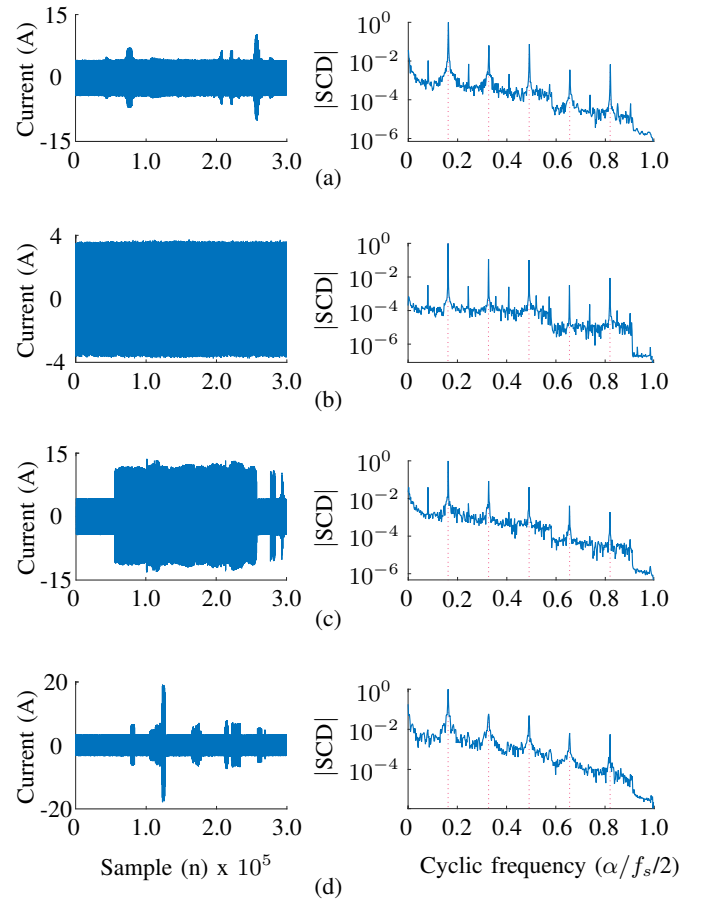


Fig. 2. HIF current and  $\alpha$ -profile for different contact surfaces, such as (a) sand, (b) gravel, (c) asphalt and (d) pavement.

#### B. Performance Assessment with Simulations

The performance of the proposed method was also assessed with simulations by considering a complex distribution system shown in Fig. 3, which is the IEEE 30-bus test system composed of 30 buses, 41 lines, and a sub-transmission and distribution system [23]. The IEEE 30-bus distribution system

was divided into three sectors, where each sector contains five busses. These sectors are highlighted with different colors in Fig. 3.

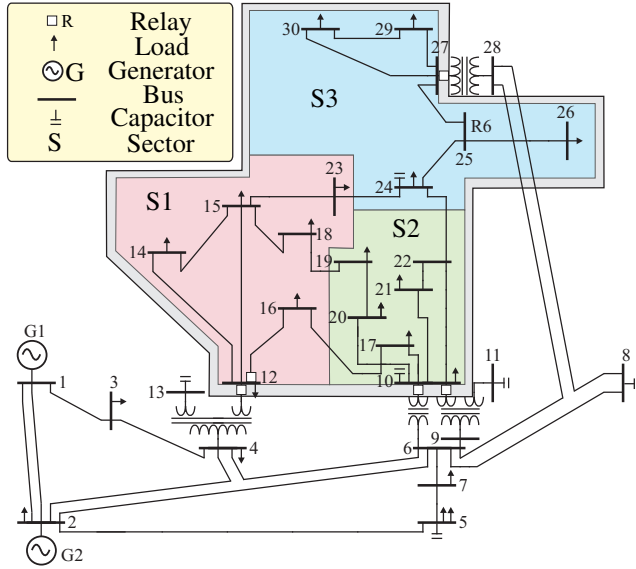


Fig. 3. IEEE 30bus distribution system.

A key point to evaluate a HIF detection method under simulation is to consider a realistic and accurate HIF model. This paper considers the HIF model proposed by [24], which is a realistic HIF model based on experimental tests. This model, shown in Fig. 4, uses two time-varying resistors in series with a single switch, where the resistance  $R_1$  presents non-linearity and asymmetry characteristics, whereas the resistance  $R_2$  implements shoulder and buildup characteristics. A switch was also used to emulate a conductor rupture. Besides, this model considers different parameters for different HIFs. Therefore, HIFs occurring in different contact environments such as gravel, pavement, and grass were performed in each line of the IEEE 30 Bus distributed system in Fig. 3, totaling 18 HIFs per sector. A relay was positioned in each substation as shown in Fig. 3 in order to cover the HIF detection in the respective sector.

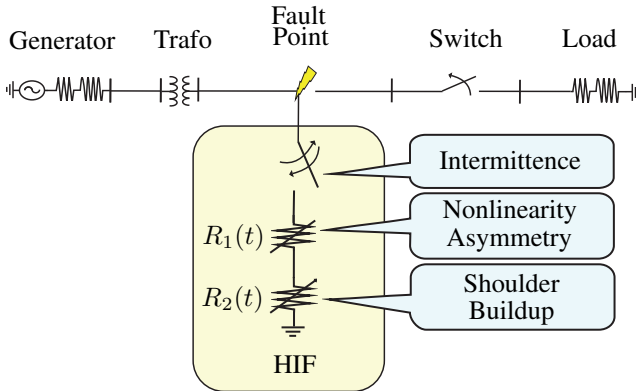


Fig. 4. HIF Model.

Besides HIFs, single phase-to-ground, double-phase, and three-phase faults were also simulated at the same places where HIFs were simulated. The fault resistance was 1  $\Omega$ ,

and a total of 18 faults per sector were simulated. Besides, capacitor bank switching and load inputs were also performed, varying the inception angle as  $0^\circ$ ,  $45^\circ$ ,  $90^\circ$ ,  $135^\circ$  and  $180^\circ$  in four different locations in each sector in the system shown in Fig. 3, totaling 20 switching events per sector.

As aforementioned, there is a relay in each sector with the proposed HIF detection method. The main goal of each relay is to detect HIFs in the respective sector. However, the performance of each relay to HIFs in other sections was also assessed. Table II summarises the performance of the proposed HIF detection method, per sector, for the simulated events.

TABLE II  
PERFORMANCE OF THE PROPOSED HIF DETECTION METHOD.

Position of the relay	Disturbance Location and Type					
	S1		S2		S3	
	HIF	Other	HIF	Other	HIF	Other
S1	100%	100%	39%	100%	0%	100%
S2	7%	100%	83%	100%	0%	100%
S3	100%	100%	100%	100%	100%	100%

Other: other disturbances.

The proposed method in the sector S1 identified 100% of HIFs, and all other disturbances were not detected as HIF in its sector. As an extra performance, it also identified 39% of HIFs in sector 2.

The proposed method in the sector S2 identified 83% of HIFs, and all other disturbances were not detected as HIF in its sector. As an extra performance, it also identified 7% of HIFs in sector 1. Fig. 5 depicts waveforms of some currents and their respective  $\alpha$  profiles for a given HIF signal located between the bars 21-22, which were evaluated at three distinct points of the subsystem, where the relays are respectively located in sectors 1, 2 and 3. These HIF currents did not present the temporal characteristics common to HIF signals. However, in the cyclic frequency domain, the proposed method could identify the HIF features in the three sectors.

The proposed method in the sector S3 identified 100% of HIFs in all sectors, and all other disturbances were not detected as HIF in this sector. Considering the cross-detection between sectors, the proposed method identified 100% of HIFs in the IEEE 30 bus system, whereas it did not identify any other disturbance as HIF.

### C. Comparison with the Conventional Overcurrent Protection

The conventional overcurrent protection with phase and neutral units was also implemented and evaluated to be compared to the proposed method. The activation of the overcurrent protection occurs when the system current reaches a value equal to or greater than a pickup current. This pickup current is given by a threshold multiplied by the reference current (steady-state current):

$$I_{50,50N,51,51N} \geq N_{50,50N,51,51N} I_r, \quad (15)$$

where  $N_{50}$  and  $N_{50N}$  are thresholds used for the instantaneous phase and neutral units; and  $N_{51}$  and  $N_{51N}$  are thresholds used for the phase and neutral time units, respectively. To perform the simulations to evaluate the performance of the conventional

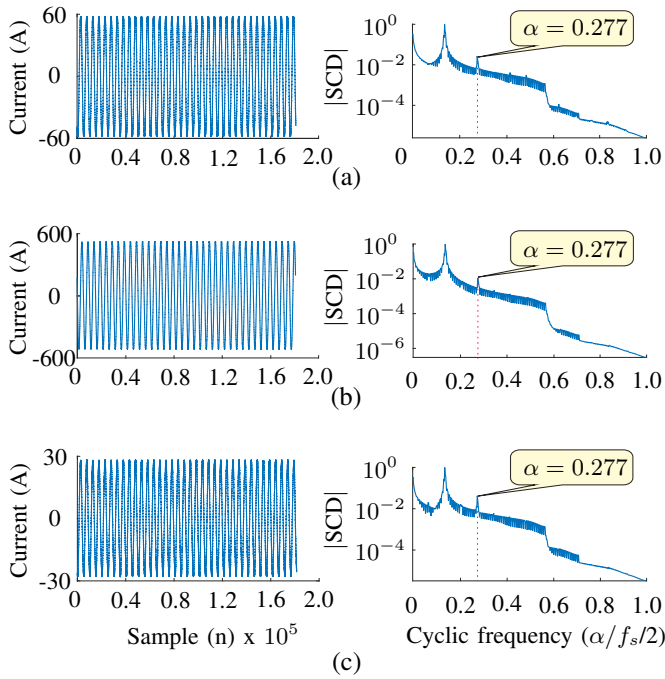


Fig. 5. Current and  $\alpha$ -profile for a HIF between bars 21-22 analyzed in each sector: (a) sector 1, (b) sector 2, (c) sector 3.

protection based on the overcurrent, the threshold values were established as summarized in Table III [25].

TABLE III  
THRESHOLD VALUES FOR OVERCURRENT PROTECTION

$N_{50}$	$N_{50N}$	$N_{51}$	$N_{51N}$
5,0	1,3	3,0	0,35

The system current upon reaching the pickup current will activate the instantaneous unit, in which the protection will act quickly, or activate the time-delay unit, which in this case will take a certain time to act.

The overcurrent protection relays were also positioned in the same places as the proposed method to protect sectors 1, 2, and 3 in Fig. 3. The success rate of the overcurrent protection, per sector, for the faults and HIFs used to evaluate the performance of the proposed method is summarized in Tables IV and V. The conventional overcurrent protection achieved a success rate of 100% for the fault detection. However, no HIF was detected in sector 1, and only 50% and 38.9% of HIFs were detected in sectors 2 and 3, respectively. Therefore, as expected, the proposed method presented better detection of HIFs (Table II) than the conventional overcurrent protection (Tables IV and V).

One advantage of the conventional overcurrent protection is that it detects faults in distribution lines with great performance and can detect some HIFs. However, the limited detected HIFs cannot be distinguished from faults. Conversely, the proposed method was designed to detect only HIFs with improved performance. Therefore, the combination of the proposed HIF detection method with the conventional overcurrent

TABLE IV  
PERFORMANCE OF THE OVERCURRENT PROTECTION - PHASE UNIT.

Position of the relay	Disturbance Location and Type					
	S1		S2		S3	
	HIF	Fault	HIF	Fault	HIF	Fault
S1	0%	100%	16.7%	83.3%	0%	5.5%
S2	0%	55.5%	0%	50%	0%	44.4%
S3	0%	100%	0%	100%	16.7%	100%

TABLE V  
PERFORMANCE OF THE OVERCURRENT PROTECTION - NEUTRAL UNIT.

Position of the relay	Disturbance Location and Type					
	S1		S2		S3	
	HIF	Fault	HIF	Fault	HIF	Fault
S1	0%	33.3%	50.0%	33.3%	0%	16.7%
S2	0%	33.3%	0%	33.3%	0%	33.3%
S3	0%	33.3%	0%	33.3%	38.9%	33.3%

functions would be interesting for the protection of distribution lines against both faults and HIFs.

#### D. Computational Burden in DSP Architecture

Considering  $N=512$ ,  $L=28$ , and  $f_s=720$  Hz, based on Table I, the total number of FLOPs in the CPD algorithm necessary to estimate the SCD function of a HIF signal formed by  $L$  blocks, each of them with  $N$  samples, is equal to  $LN(4N + 3\log_2 N) + N(N + 1)=30$  million FLOPs. From the HIF inception time, each block requires  $N/f_s=0.7111$  seconds, whereas the total signal window requires  $L.N/f_s=19.9111$  seconds.

In a real time evaluation, the computational burden of 30 million FLOPs can be accomplished from 19.9111 seconds after the HIF inception time. Considering the DSP TMS320C6748, which performs up to 2746 MFLOPS (million floating-point operations per second) [26], the computation of the SCD function for an actual HIF signal would take approximately 11 ms. Therefore, the HIF would be identified approximately  $19.9111+0.011=19.922$  seconds from its inception time. However, Eqs. (8) and (9) can run from the building of each block (from 0.7111,  $2*0.7111$ , ...,  $28*0.7111$  seconds of the HIF inception time) instead from 19.9111 seconds of the HIF inception time, i.e., the computational burden of 30 million FLOPs can be partitioned and accomplished during the data acquisition, speeding up the HIF identification process and making possible the usage of less powerful DSPs.

Considering that most HIFs are not detected by conventional protective relays, and when detected the relay operating time can take up to several minutes, then if a particular DSP is not able to run the proposed method in 0.011 seconds it can take extra time with no problem because, in this context, the correct detection of HIF is more important than a high-speed HIF detection.

#### E. Effect of Noise

The noise in power systems is usually a white Gaussian additive one. Although intrinsic to any measurement process,

noise becomes a critical point in detecting disturbances with damped transients, such as HIFs, especially when the noise intensity is relevant. Fortunately, the cyclostationary technique presents robustness to signal effected by white Gaussian additive noise. The cyclostationary analysis is based on extracting cyclostationary characteristics of signals using the correlation of the analyzed signal in the frequency domain. The correlation of noise at a non-zero cyclic frequency approaches zero. In this way, the noise has a minimized influence in the cycle analysis.

As aforementioned, the simulations of the previous cases were performed with an SNR of 60 dB. Therefore, the same disturbances described in the previous section were considered with 30 dB and 40 dB to evaluate the effect of noise in the performance of the proposed method. The proposed method presented a success rate of 100% regardless of the noise level, demonstrating its remarkable robustness even with severe noise signals.

Fig. 6 depicts waveforms of a HIF and its corresponding  $\alpha$  profiles with a noise level of 60 dB, 40 dB, and 30 dB, demonstrating that the noise does not affect the proposed method. In fact, while most other methods are affected by the noise [1], an advantage of the cyclostationary analysis is that the extraction of characteristics can be performed even under noise-corrupted signals, such as with 30 dB SNR, which is considered critical for noise.

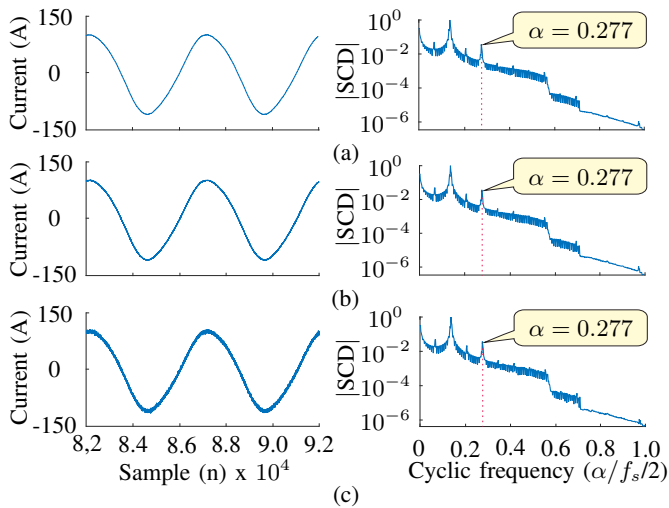


Fig. 6. Currents and Alpha Profiles of a HIF with the addition of noise (a) 60 dB, (b) 40 dB and (c) 30 dB.

## VI. CONCLUSIONS

This work proposed a method based on the cyclostationary technique to identify HIFs in distribution power systems. The cyclostationary analysis was used to extract the cyclostationary characteristics of the analyzed signal using the cyclic spectral density function. Alpha profiles were generated from the cyclostationary characteristics to be used in the classification of disorders present in the distribution system.

The proposed method was evaluated with simulations from a complex electric power distribution test system considering different disturbances such as HIFs, faults with overcurrent, transformer energization, capacitor bank switching, and non-linear loads. The proposed method presented outstanding results with 100% of success rate. The proposed method was

also assessed with actual data from tests carried out in an actual distribution power system, presenting a success rate of 100%. Whereas most of the literature methods present some difficulty for identifying HIFs because the transients induced by HIFs are damped and near the noise level and the low amplitude current, the proposed method can treat current signals with low SNR levels since the cyclostationary analysis minimizes the influence of the noise present in the signal. Besides, the low-level of overcurrent was not an issue for the proposed method.

The conventional overcurrent protection obtained 100% of success rate for detecting faults. However, it failed to detect most of the simulated HIFs as expected. Failure to operate conventional protection has caused some HIFs to remain for hours. Therefore, the combination of the proposed method with the conventional one could be an interesting possibility to protect the distribution system against both faults and HIF. Also, this paper demonstrates that the proposed method might be possible to be implemented in modern digital signal processors.

## REFERENCES

- [1] F. B. Costa, B. A. Souza, N. S. D. Brito, J. A. C. B. Silva, and W. C. Santos. Real-time detection of transients induced by high-impedance faults based on the boundary wavelet transform. *IEEE Transactions on Industry Applications*, 51(6):5312–5323, 2015.
- [2] ABRADÉE. Associação Brasileira de Distribuição de Energia. XIII semana nacional da segurança da população com energia elétrica. <http://www.abradee.com.br/>, 2019 (accessed 30 July 2019).
- [3] A. N. Milioudis, G. T. Andreou, and D. P. Labridis. Enhanced protection scheme for smart grids using power line communications techniques—part i: Detection of high impedance fault occurrence. *IEEE Transactions on Smart Grid*, 3(4):1621–1630, 2012.
- [4] H. Yeh, S. Sim, and R. J. Bravo. Wavelet and denoising techniques for real-time hif detection in 12-kv distribution circuits. *IEEE Systems Journal*, 13(4):4365–4373, 2019.
- [5] A. Ghaderi, H. A. Mohammadpour, H. Ginn, and Yong-June Shin. High impedance detection in distribution network using time-frequency based algorithm. In *2015 IEEE Power Energy Society General Meeting*, pages 1–1, 2015.
- [6] S. Gautam and S. M. Brahma. Detection of high impedance fault in power distribution systems using mathematical morphology. *IEEE Transactions on Power Systems*, 28(2):1226–1234, 2013.
- [7] M. Kavi, Y. Mishra, and M. D. Vilathgamuwa. High-impedance fault detection and classification in power system distribution networks using morphological fault detector algorithm. *IET Generation, Transmission Distribution*, 12(15):3699–3710, 2018.
- [8] S. R. Samantaray and P. K. Dash. High impedance fault detection in distribution feeders using extended kalman filter and support vector machine. *European Transactions on Electrical Power*, 20(3):382–393, 2010.
- [9] A. H. Etemadi and M. Sanaye-Pasand. High-impedance fault detection using multi-resolution signal decomposition and adaptive neural fuzzy inference system. *IET generation, transmission & distribution*, 2(1):110–118, 2008.
- [10] M. Y. Suliman and M. T. Ghazal. Detection of high impedance fault in distribution network using fuzzy logic control. In *2019 2nd International Conference on Electrical, Communication, Computer, Power and Control Engineering (ICECCPCE)*, pages 103–108, 2019.
- [11] S. Wang and P. Dehghanian. On the use of artificial intelligence for high impedance fault detection and electrical safety. *IEEE Transactions on Industry Applications*, 56(6):7208–7216, 2020.
- [12] W. A. Gardner. Cyclostationarity in communications and signal processing. Technical report, STATISTICAL SIGNAL PROCESSING INC YOUNTVILLE CA, 1994.
- [13] R. F. Schkoda, R. B. Lund, and J. R. Wagner. Clustering of cyclostationary signals with applications to climate station sitings, eliminations, and merges. *IEEE Journal of Selected Topics in Applied Earth Observations and Remote Sensing*, 7(5):1754–1762, 2014.

- [14] T. V. R. O. Câmara, A. D. L. Lima, B. M. M. Lima, A. I. R. Fontes, A. D. M. Martins, and L. F. Q. Silveira. Automatic modulation classification architectures based on cyclostationary features in impulsive environments. *IEEE Access*, 7:138512–138527, 2019.
- [15] W. A. Gardner, A. Napolitano, and L. Paura. Cyclostationarity: Half a century of research. *Signal processing*, 86(4):639–697, 2006.
- [16] W. A. Gardner. Exploitation of spectral redundancy in cyclostationary signals. *IEEE Signal Processing Magazine*, 8(2):14–36, 1991.
- [17] A. D. L. Lima. Arquiteturas eficientes para sensoriamento espectral e classificação automática de modulações usando características cicloestacionárias. Master's thesis, Universidade Federal do Rio Grande do Norte, 2014.
- [18] Z. Zhang and X. Xu. Implementation of cyclic periodogram detection on vee for cognitive radio. In *Global Mobile Congress, Mobile World Congress Shanghai*, pages 1–5, 2007.
- [19] F. B. Costa. Boundary wavelet coefficients for real-time detection of transients induced by faults and power-quality disturbances. *IEEE Transactions on Power Delivery*, 29(6):2674–2687, 2014.
- [20] F. B. Costa and J. Driesen. Assessment of voltage sag indices based on scaling and wavelet coefficient energy analysis. *IEEE Trans. Power Del.*, 28(1):336–346, Jan. 2013.
- [21] F. B. Costa. Fault-induced transient detection based on real-time analysis of the wavelet coefficient energy. *IEEE Trans. Power Del.*, 29(01):140–153, Fev. 2014.
- [22] P. E. Danielsson. Euclidean distance mapping. *Computer Graphics and image processing*, 14(3):227–248, 1980.
- [23] R. Yokoyama, S. H. Bae, T. Morita, and H. Sasaki. Multiobjective optimal generation dispatch based on probability security criteria. *IEEE Transactions on Power Systems*, 3(1):317–324, 1988.
- [24] W. C. Santos, B. A. Souza, N. S. D. Brito, F. B. Costa, and M. R. C. Paes. High impedance faults: From field tests to modeling. *Journal of Control, Automation and Electrical Systems*, 24(6):885–896, 2013.
- [25] F. B. Costa, A. Monti, and S. C. Paiva. Overcurrent protection in distribution systems with distributed generation based on the real-time boundary wavelet transform. *IEEE Transactions on Power delivery*, 32(1):462–473, 2015.
- [26] Texas Instruments. *TMS320C6748™ Fixed- and Floating-Point DSP Datasheet*, 2009 [Revised 2017].